

# Synthesis of Highly Selective Indole-Based Sensors for Mercuric Ion

Huei-Jyun Huang · Jiun-Ly Chir · Hsiu-Jung Cheng ·  
Shau-Jiun Chen · Ching-Han Hu · An-Tai Wu

Received: 15 October 2010 / Accepted: 28 December 2010 / Published online: 15 January 2011  
© Springer Science+Business Media, LLC 2011

**Abstract** Two indole-based fluorescent chemosensors **1** and **2** were prepared and investigated characteristic features with transition metal ions. Sensors **1** and **2** were selective for  $\text{Hg}^{2+}$  ion, among a series of metal ions, in aqueous ethanol ( $\text{H}_2\text{O}$ –EtOH, 1:2, v/v) with association constants of  $5.74 \times 10^3$  and  $4.46 \times 10^3 \text{ M}^{-1}$  and detection limits of 7.4 and 6.8  $\mu\text{M}$ , respectively. Computational results revealed that sensor **1** or **2** with  $\text{Hg}^{2+}$  ion formed 1:1 complex with a central, sandwich-coordinated  $\text{Hg}^{2+}$  ion. Computational calculations provided evidence that a sandwich-coordinated  $\text{Hg}^{2+}$  ion center was formed and the polyoxyethylene spacer acted as a scaffold for bringing functional ligands into a suitable geometry.

**Keywords** Chemosensor · Indole · Fluorescence ·  $\text{Hg}^{2+}$  ion

The design and synthesis of new chemosensors for efficient detection of trace metal ions is among the most important research topics in environmental chemistry and biology [1]. For example, mercuric ion ( $\text{Hg}^{2+}$ ) is a significant environmental pollutant that accumulates in plants, soil, and water. In the marine environment,  $\text{Hg}^{2+}$  ion is converted by bacteria into toxic methylmercury, a highly potent neurotoxin, and is passed up the food chain to accumulate in humans [2]. Therefore, it is very important to develop

highly sensitive assays for detecting  $\text{Hg}^{2+}$  ion [3, 4]. In recent years, several chemosensors specific for  $\text{Hg}^{2+}$  ion have been developed [5–9]; however, most of these sensors required complicated synthesis. For practical applications, it is necessary to develop sensors that are easily prepared and possess selective and sensitive signaling mechanisms. Recently, simple indole derivatives were developed as potential fluorescent chemosensors for  $\text{Ag}^+$  ion [10]. The inherent fluorescent property of the indole chromophore is sensitive to changes in the local environment [11–16]. Therefore, exploring the potential of the indole moiety should provide promising results in the design of fluorescent chemosensors for metal ions. In this study, we combined indole-3-acetic acid (IAA) with polyoxyethylenes to synthesize two indole-based fluorescent chemosensors **1** and **2** for metal-ion screening studies. Both of these IAA-appended chemosensor exhibited selectivity and sensitivity for  $\text{Hg}^{2+}$  ion compared to other transition and heavy metal ions in aqueous ethanol.

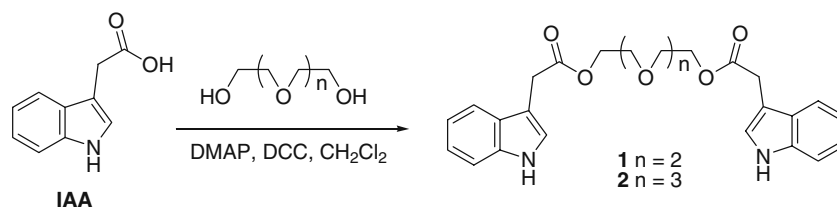
## Experimental

### Apparatus

The  $^1\text{H}$  and  $^{13}\text{C}$  NMR spectra were recorded with Bruker AM 300 (300 MHz) spectrometers. Chemical shifts are expressed in ppm with residual  $\text{CHCl}_3$  as reference. Low- and high-resolution mass spectra were recorded under fast atom bombardment (FAB) conditions. UV–vis spectra were recorded by using HP-8453 spectrophotometer with a diode array detector, and there solution was set at 1 nm. Fluorescence spectra were recorded on a Cary Eclipse Fluorescence spectrophotometer.

**Electronic supplementary material** The online version of this article (doi:10.1007/s10895-010-0804-0) contains supplementary material, which is available to authorized users.

H.-J. Huang · J.-L. Chir · H.-J. Cheng · S.-J. Chen · C.-H. Hu ·  
A.-T. Wu (✉)  
Department of Chemistry,  
National Changhua University of Education,  
Changhua 50058, Taiwan  
e-mail: antai@cc.ncue.edu.tw

**Scheme 1** Synthesis of chemosensors **1** and **2****Reagents**

Compound **1** and **2** were synthesized in one step as shown in Scheme 1.

2,2'-(ethane-1,2-diylbis(oxy))bis(ethane-2,1-diyl) bis(2-(1H-indol-3-yl)acetate) (**1**)

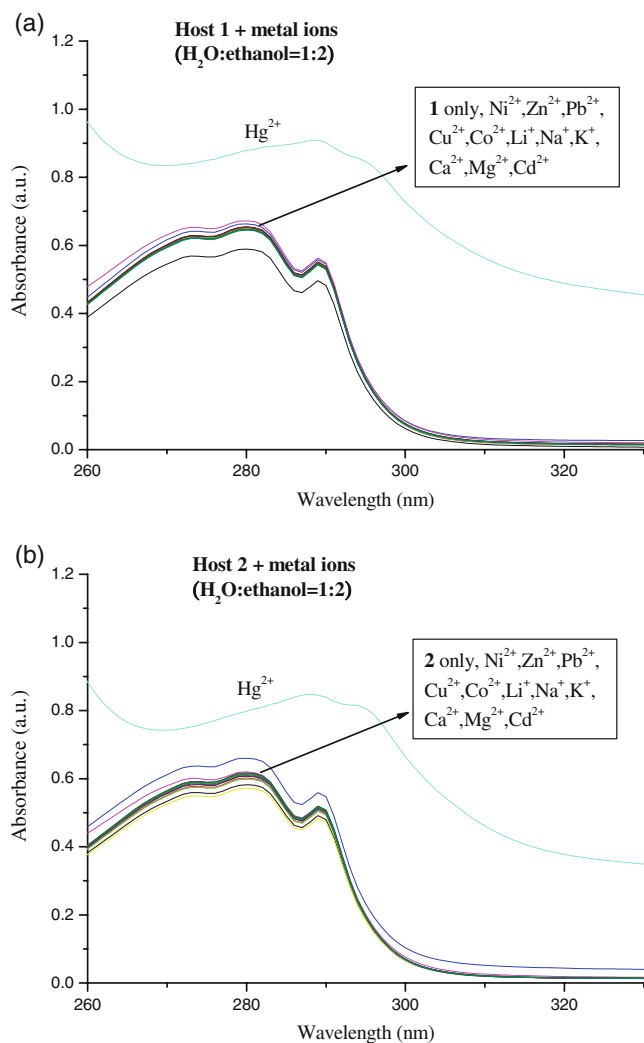
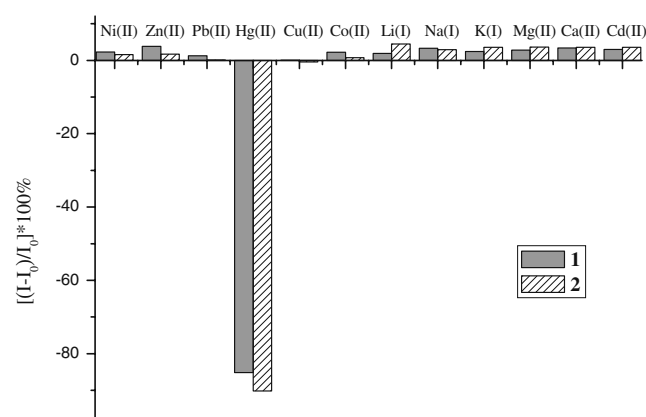
To a stirred solution of 3-Indolacetic acid (0.66 g, 3.7 mmol) in dry  $\text{CH}_2\text{Cl}_2$  (15 mL) was added DMAP

(2.20 g, 17.9 mmol), DCC (3.78 g, 18.3 mmol), and triethylene glycol (0.2 mL, 1.5 mmol). The reaction mixture was stirred overnight at room temperature. The mixture was filtered and the filtrate washed with 1 M HCl, water, aq  $\text{NaHCO}_3$  and brine, dried and concentrated. The resulting residue was purified by silica column chromatography (Hexane/EtOAc=1:5) to give **1** (0.62 g, 86%) as a sorrel jelly;  $R_f=0.62$  (Hexane/EtOAc=1:10);  $^1\text{H NMR}$  (300 MHz,  $\text{CDCl}_3$ )  $\delta$ : 8.226 (s, 2 H), 7.60–7.57 (m, 2 H), 7.28–7.25 (m, 2 H), 7.18–7.11 (m, 4 H), 7.03 (d,  $J=2.1$  Hz, 2 H), 4.25–4.20 (m, 4 H), 3.76 (d,  $J=0.6$  Hz, 4 H), 3.62–3.58 (m, 4 H), 3.46 (s, 4 H);  $^{13}\text{C NMR}$  (75 MHz,  $\text{CDCl}_3$ )  $\delta$ : 172.10, 136.02, 127.12, 123.25, 122.01, 119.49, 118.75, 111.20, 107.99, 70.34, 69.01, 63.82, 31.27; HRMS (FAB): Calcd for  $\text{C}_{26}\text{H}_{29}\text{N}_2\text{O}_6$  (M+H),  $m/z$  465.2026, found  $m/z$  465.2038.

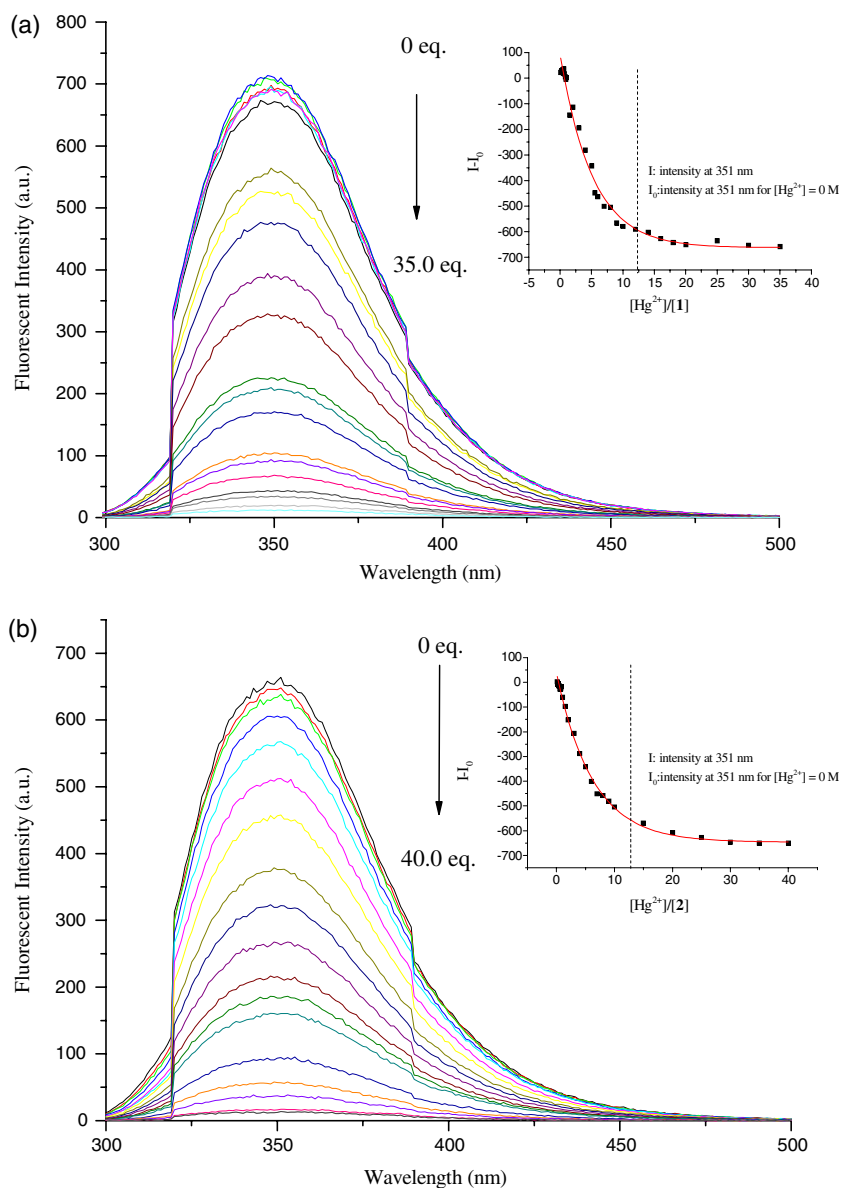
2,2'-(2,2'-oxybis(ethane-2,1-diyl)bis(oxy))bis(ethane-2,1-diyl) bis(2-(1H-indol-3-yl)acetate) (**2**)

The same procedures as described above were used to obtain **2** (85%) as a yellow oil.

$R_f=0.53$  (Hexane/EtOAc=1:10);  $^1\text{H NMR}$  (300 MHz,  $\text{CDCl}_3$ )  $\delta$ : 8.35 (s, 2 H), 7.57 (d,  $J=7.5$  Hz, 2 H), 7.29 (d,  $J=7.8$  Hz, 2 H), 7.18–7.06 (m, 6 H), 4.28–4.25 (m, 4 H), 3.75 (s, 4 H), 3.66–3.64 (m, 4 H), 3.52 (s, 8 H);  $^{13}\text{C NMR}$  (75 MHz,  $\text{CDCl}_3$ )  $\delta$ : 172.03, 135.83, 126.80, 123.37, 121.47, 118.99, 118.33, 111.13, 107.12, 70.01, 68.60, 63.52, 30.91; HRMS (FAB): Calcd for  $\text{C}_{28}\text{H}_{33}\text{N}_2\text{O}_7$  (M+H),  $m/z$  509.2288, found  $m/z$  509.2289.

**Fig. 1** UV-vis spectra of **a 1** (50  $\mu\text{M}$ ) and **b 2** (50  $\mu\text{M}$ ) upon the addition of  $\text{Li}^+$ ,  $\text{Na}^+$ ,  $\text{K}^+$ ,  $\text{Ca}^{2+}$ ,  $\text{Mg}^{2+}$ ,  $\text{Hg}^{2+}$ ,  $\text{Co}^{2+}$ ,  $\text{Ni}^{2+}$ ,  $\text{Zn}^{2+}$ ,  $\text{Cu}^{2+}$ ,  $\text{Cd}^{2+}$ , and  $\text{Pb}^{2+}$  (10 equiv) in  $\text{H}_2\text{O}$ : EtOH (1:2, v/v) (excitation at 280 nm)**Fig. 2** Fluorescence intensity changes ( $(I-I_0)/I_0 \times 100\%$ ) of **1** (50  $\mu\text{M}$ ) and **2** (50  $\mu\text{M}$ ) upon the addition of  $\text{Li}^+$ ,  $\text{Na}^+$ ,  $\text{K}^+$ ,  $\text{Ca}^{2+}$ ,  $\text{Mg}^{2+}$ ,  $\text{Hg}^{2+}$ ,  $\text{Co}^{2+}$ ,  $\text{Ni}^{2+}$ ,  $\text{Zn}^{2+}$ ,  $\text{Cu}^{2+}$ ,  $\text{Cd}^{2+}$ , and  $\text{Pb}^{2+}$  (10 equiv) in  $\text{H}_2\text{O}$ : EtOH (1:2, v/v) (excitation at 280 nm)

**Fig. 3** Fluorescence spectra of **a 1** (74.0  $\mu\text{M}$ ) and **b 2** (68.3  $\mu\text{M}$ ) in the presence of different concentrations of the  $\text{Hg}^{2+}$  ion in  $\text{H}_2\text{O}$ : EtOH (1:2, v/v) with an excitation at 280 nm



## Procedure

Typically, to a 10-mL test tube containing 6.6 mL ethanol, and 0.1 mL of compound **1** or **2**, an appropriate aliquot of  $\text{Hg}^{2+}$  ion was added and the reaction mixture was diluted to 10.0 mL with water. The resulting solution was allowed to stand at room temperature for 30 min, and then the absorption and emission spectra were recorded. For fluorescence intensity measurements, the excitation and emission wavelengths were at 280 nm and 351 nm, respectively.

## Results and Discussion

Figure 1a shows that the absorption band of **1** in the UV–vis spectrum originally appears at 280 nm in a solution of  $\text{H}_2\text{O}$ –

EtOH (1:2, v/v). After addition of 10 equivalents of the following 12 metal ions:  $\text{Li}^+$ ,  $\text{Na}^+$ ,  $\text{K}^+$ ,  $\text{Ca}^{2+}$ ,  $\text{Mg}^{2+}$ ,  $\text{Hg}^{2+}$ ,  $\text{Co}^{2+}$ ,  $\text{Ni}^{2+}$ ,  $\text{Cu}^{2+}$ ,  $\text{Pb}^{2+}$ ,  $\text{Cd}^{2+}$  and  $\text{Zn}^{2+}$ , only the  $\text{Hg}^{2+}$  ion had a larger molar absorption coefficient than the original one, while other ions did not cause any significant changes under identical condition. In comparison of **1**, **2** also has the similar results in the UV–vis spectrum (Fig. 1b). The molar absorptivities are  $1.09 \times 10^4$  and  $1.07 \times 10^4 \text{ M}^{-1} \text{ cm}^{-1}$  for **1** and **2**, respectively. The results may be due to the intermolecular interactions between **1** or **2** and  $\text{Hg}^{2+}$  ion by  $\text{Hg}^{2+}$  ion complexation-induced changes in UV–vis absorption. The chemosensor behavior was also investigated by the fluorescence measurement in a solution of  $\text{H}_2\text{O}$ –EtOH (1:2, v/v) upon excitation at 280 nm. The excitation and emission spectra were also recorded (Figure S1). The results indicated that the fluorescence

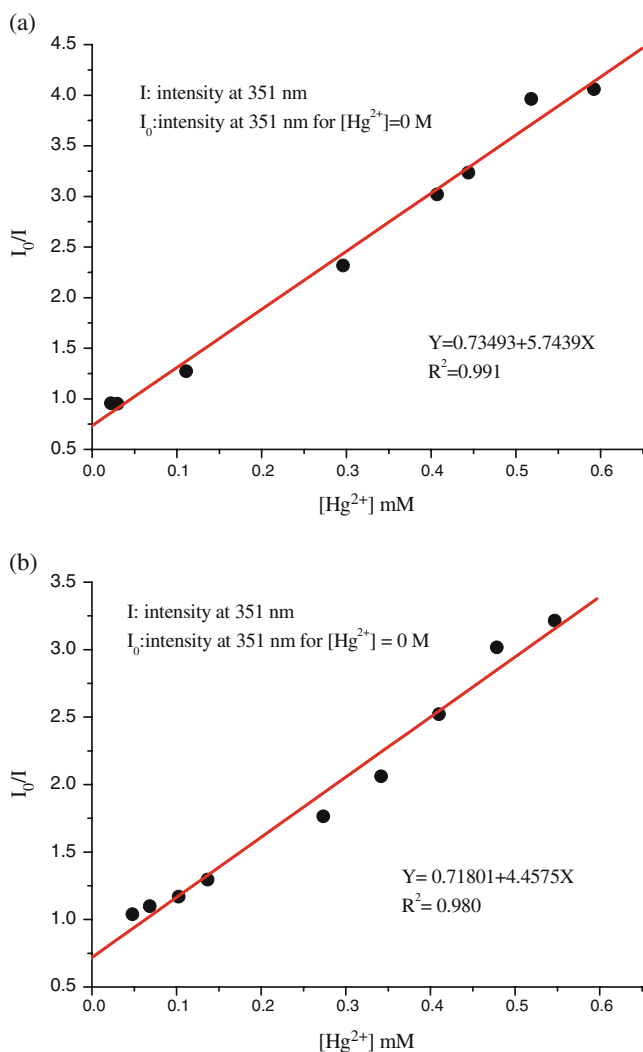


**Fig. 4** Stern-Volmer plot of **a 1** and **b 2** with  $Hg(ClO_4)_2$

intensity of **1** was strongly quenched in the presence of the  $Hg^{2+}$  ion in  $H_2O$ -EtOH (1:2 v/v) (Figure S2), where presence of other metal ions did not affect the fluorescence intensity of **1** significantly. Similarly, selective quenching by  $Hg^{2+}$  ion was also observed for compound **2** (Figure S3). For **1**, the observed quenching efficiency ( $(I - I_0/I_0) \times 100\%$ ) at 351 nm was nearly 85% (Fig. 2) where the other metal ions caused small enhancement in fluorescence intensity. For **2**, the quenching efficiency was 90% (Fig. 2) where the other metal ions also caused small enhancement in fluorescence intensity. These results indicated that the length of polyoxyethylene spacer could not influence the binding of  $Hg^{2+}$  to the **1** or **2**. To further investigate the chemosensing properties of **1** and **2**, we performed fluorescence titrations of **1** (74.0  $\mu M$ ) and **2** (68.3  $\mu M$ ) in the presence of different concentrations of  $Hg^{2+}$  ion in  $H_2O$ -EtOH (1:2 v/v).

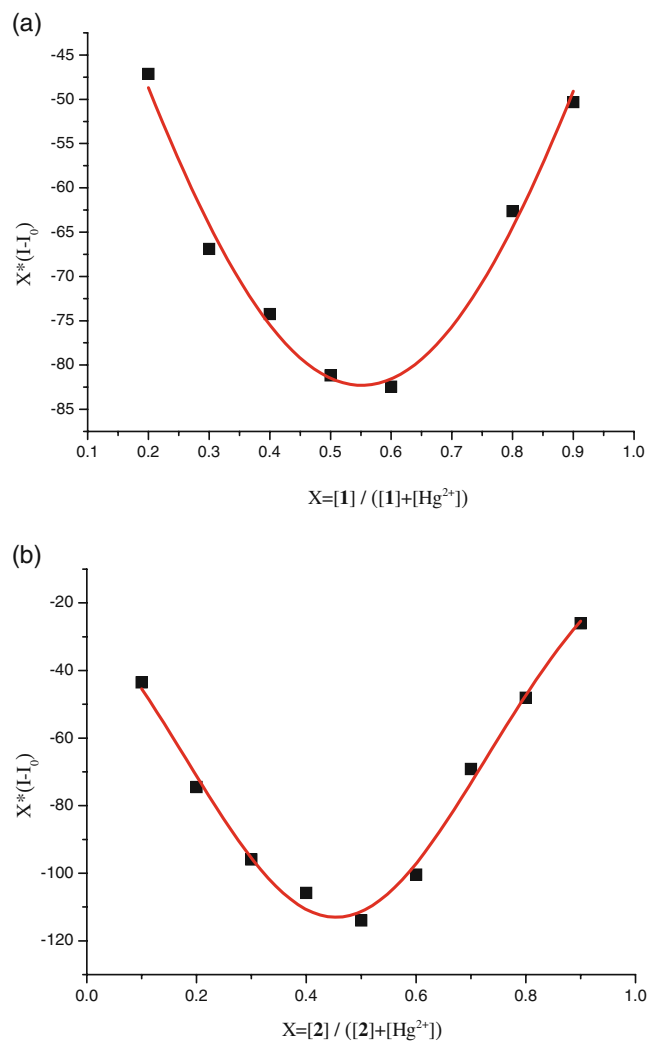


**Fig. 5** Job's plot of **a 1** and **b 2** with  $Hg^{2+}$  in  $H_2O$ : EtOH (1:2, v/v)

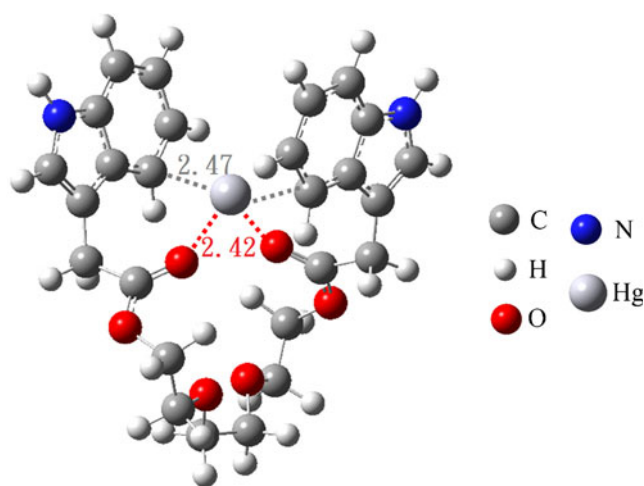


**Fig. 6** Conformation of **1**/ $Hg^{2+}$  optimized by density functional theory

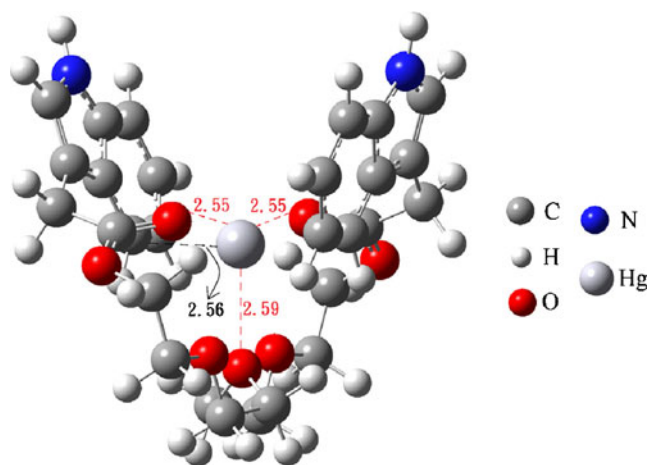


**Fig. 7** Conformation of  $2/\text{Hg}^{2+}$  optimized by density functional theory

Figure 3a and b show the gradual reductions in fluorescence intensity for **1** and **2** upon addition of increasing concentrations of  $\text{Hg}^{2+}$ . From the fluorescence titration profiles, the association constants for  $1 \cdot \text{Hg}^{2+}$  and  $2 \cdot \text{Hg}^{2+}$  were found to be  $5.74 \times 10^3$  and  $4.46 \times 10^3 \text{ M}^{-1}$ , respectively, according to the Stern-Volmer plot (Fig. 4).

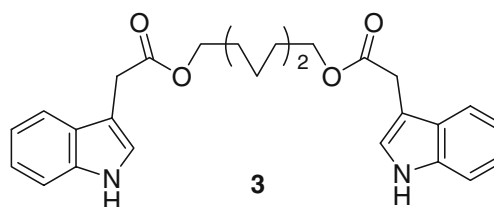
By using above-mentioned fluorescence titration results, the detection limits for  $\text{Hg}^{2+}$  ion were 7.4 and 6.8  $\mu\text{M}$  for **1** and **2**, respectively. In the Job's plot (Fig. 5a and b), a maximum fluorescence change was observed with a 0.5 molar fraction of ionophore to  $\text{Hg}^{2+}$  for **1** or **2**, which indicated the forming of a 1:1 complex. Selectivity for the  $\text{Hg}^{2+}$  ion was further ascertained with competition experiments (Figures S4 and S5). We found that the fluorescence intensity of **1** and **2** in the presence of 10 equivalents of  $\text{Hg}^{2+}$  ion was unaffected by the addition of 10 equivalents of competing metal ions ( $\text{Li}^+$ ,  $\text{Na}^+$ ,  $\text{K}^+$ ,  $\text{Ca}^{2+}$ ,  $\text{Mg}^{2+}$ ,  $\text{Co}^{2+}$ ,  $\text{Ni}^{2+}$ ,  $\text{Cu}^{2+}$ ,  $\text{Pb}^{2+}$ ,  $\text{Cd}^{2+}$ , or  $\text{Zn}^{2+}$ ).

Free IAA has a broad selectivity for transition metal ions (i.e.,  $\text{Hg}^{2+}$ ,  $\text{Cu}^{2+}$ , and  $\text{Pb}^{2+}$ , respectively. Figure S6); however, **1** and **2** have an extremely specific selectivity for  $\text{Hg}^{2+}$  ion. To better understand the coordination behavior of **1** and **2** with  $\text{Hg}^{2+}$  ion, we conducted  $^1\text{H}$  NMR experiments. When compound **1** or **2** was prepared in the  $\text{D}_2\text{O}$ –EtOD solution (1:2 v/v), we did not detect any clear changes in the  $^1\text{H}$  chemical shift of **1** or **2** upon addition of  $\text{Hg}^{2+}$  ions (Figure S7).

To further investigate coordinating mode of the  $1\text{-Hg}^{2+}$  and  $2\text{-Hg}^{2+}$  complex, computations for  $1\text{-Hg}^{2+}$  and  $2\text{-Hg}^{2+}$  were conducted at the B3LYP/LanL2DZ theory level with a Gaussian 03 package. On the basis of these calculations of  $1\text{-Hg}^{2+}$  complex, we found four stationary points that could be verified as genuine minima via vibrational frequency analyses. The optimized structure for the most stable isomer

of  $1\text{-Hg}^{2+}$  is illustrated in Fig. 6. It is clear that the  $\text{Hg}^{2+}$  ion occupied the coordination center of **1**, surrounded by two carbonyl groups and two anti-parallel indole rings. The average bond length of  $\text{Hg-O=C}$  was estimated at 2.42 Å, and those of  $\text{Hg-C}$  and  $\text{Hg-N}$  of the indole ring in  $1\text{-Hg}^{2+}$  were 2.47 Å and 4.78 Å, respectively. On the other hand, these calculations of  $2\text{-Hg}^{2+}$  complex, we found three stationary points that could be verified as genuine minima via vibrational frequency analyses. The optimized structure for the most stable isomer of  $2\text{-Hg}^{2+}$  is similar with  $1\text{-Hg}^{2+}$  as illustrated in Fig. 7. The average bond length of  $\text{Hg-O=C}$  was estimated at 2.56 Å, and those of  $\text{Hg-C}$  and  $\text{Hg-N}$  of the indole ring in  $2\text{-Hg}^{2+}$  were 2.55 Å and 5.04 Å, respectively. These results indicated that a sandwich-coordinated  $\text{Hg}^{2+}$  ion center was formed, where all the neighboring ligands (i.e., two carbonyl oxygen atoms and two indole rings) were involved in binding with the  $\text{Hg}^{2+}$  ion, and the polyoxyethylene spacer acted as a scaffold for bringing these functional ligands into a suitable geometry.

Another confirmation of the binding structures of **1** and **2** with  $\text{Hg}^{2+}$  ion was shown by testing a new chemosensor **3**, an analogue to **1** but with carbon instead of oxygen in the methylene spacer. The synthesis of sensor **3** was similar with sensor **1** or **2**. We found that chemosensor **3** exhibited the same binding behavior with  $\text{Hg}^{2+}$  ion as that of sensors **1** and **2**. Similarly, sensor **3** showed significant fluorescence quenching in the presence of the  $\text{Hg}^{2+}$  ion (Figure S8). These results provided support for calculated binding modes of **1** and **2** derived in the computational study.



## Conclusion

In summary two aqueous indole-based,  $\text{Hg}^{2+}$ -selective, fluorescent sensors **1** and **2** were designed and synthesized by coupling indole and ethylene glycol moieties. Both **1** and **2** showed selectivity for  $\text{Hg}^{2+}$  ion over other metal ions. Computational calculations provided evidence that a sandwich-coordinated  $\text{Hg}^{2+}$  ion center was formed and the polyoxyethylene spacer acted as a scaffold for bringing functional ligands into a suitable geometry.

**Acknowledgments** We thank the National Science Council of Taiwan for financial support.

## References

1. de Silva AP, Gunaratne HQN, Gunlaugsson T, Huxley AJM, McCoy CP, Rademacher JT, Rice TE (1997) Signaling recognition events with fluorescent sensors and switches. *Chem Rev* 97:1515–1566
2. Grandjean P, Weihe P, White RF, Debes F (1998) Cognitive performance of children prenatally exposed to “Safe” levels of methylmercury. *Environ Res* 77:165–172
3. Yuan M, Li Y, Li J, Li C, Liu X, Lv J, Xu J, Liu H, Wang S, Zhu D (2007) A colorimetric and fluorometric dual-modal assay for mercury ion by a molecule. *Org Lett* 9:2313–2316
4. Zhu M, Yuan M, Liu X, Xu J, Lv J, Huang C, Liu H, Li Y, Wang S, Zhu D (2008) Visible near-infrared chemosensor for mercury ion. *Org Lett* 10:1481–1484
5. Kao T-L, Wang C-C, Pan Y-T, Shiao Y-J, Yen J-Y, Shu C-M, Lee G-H, Peng S-M, Chung W-S (2005) Upper rim allyl- and arylazo-coupled calix[4]arenes as highly sensitive chromogenic sensors for  $\text{Hg}^{2+}$  ion. *J Org Chem* 70:2912–2920
6. Chen Q-Y, Chen CF (2005) A new  $\text{Hg}^{2+}$ -selective fluorescent sensor based on a dansyl amide-armed calix[4]-aza-crown. *Tetrahedron Lett* 46:165–168
7. Moon SY, Cha NR, Kim YH, Chang SK (2004) New  $\text{Hg}^{2+}$ -selective chromo- and fluoroionophore based upon 8-hydroxyquinoline. *J Org Chem* 69:181–183
8. Cha NR, Kim MY, Kim YH, Choe J-I, Chang S-K (2002) New  $\text{Hg}^{2+}$ -selective fluoroionophores derived from *p-tert*-butylcalix[4]arene-azacrown ethers. *J Chem Soc Perkin Trans 2*:1193–1196
9. Kumar A, Pandey PS (2009) Steroidal 1, 2, 3-triazole-based sensors for  $\text{Hg}^{2+}$  ion and their logic gate behaviour. *Tetrahedron Lett* 50:5842–5845
10. Rocha A, Marques MMB, Lodeiro C (2009) Synthesis and characterization of novel indole-containing half-crowns as new emissive metal probes. *Tetrahedron Lett* 50:4930–4933
11. Adams PD, Chen Y, Ma K, Zagorski MG, Sonnichsen FD, McLaughlin ML, Barkley MD (2002) Intramolecular quenching of tryptophan fluorescence by the peptide bond in cyclic hexapeptides. *J Am Chem Soc* 124:9278–9286
12. Liu B, Thalji RK, Adams PD, Fronczek FR, McLaughlin ML, Barkley MD (2002) Fluorescence of *cis*-1-amino-2-(3-indolyl)cyclohexane-1-carboxylic acid: a single tryptophan  $\chi_1$  rotamer model. *J Am Chem Soc* 124:13329–13338
13. Shizuka J, Serizawa M, Kobayashi J, Kameta K, Sugiyama H, Matsuura T, Saito I (1988) Excited-state behavior of tryptamine and related indoles. Remarkably efficient intramolecular proton-induced quenching. *J Am Chem Soc* 110:1726–1732
14. Sessler JL, Cho DG, Lynch V (2006) Diindolylquinoxalines: effective indole-based receptors for phosphate anion. *J Am Chem Soc* 128:16518–16519
15. He X, Hu S, Liu K, Guo Y, Xu J, Shao S (2006) Oxidized bis(indolyl)methane: a simple and efficient chromogenic-sensing molecule based on the proton transfer signaling mode. *Org Lett* 8:333–336
16. Li L, Dang YQ, Li HW, Wang B, Wu Y (2010) Fluorescent chemosensor based on Schiff base for selective detection of zinc (II) in aqueous solution. *Tetrahedron Lett* 51:618–621